

Stationary behavior of a chain of interacting spasers

E. S. Andrianov,^{1,2} A. A. Pukhov,^{1,2} A. V. Dorofeenko,^{1,2} A. P. Vinogradov,^{1,2} and A. A. Lisyansky^{3,*}

¹*Moscow Institute of Physics and Technology, 9 Institutskiy Pereulok, Dolgoprudniy 141700, Moscow Region, Russia*

²*Institute for Theoretical and Applied Electromagnetics, 13 Izhorskaya, Moscow 125412, Russia*

³*Department of Physics, Queens College of the City University of New York, Flushing, New York 11367, USA*

(Received 23 December 2011; published 9 April 2012)

We show that depending on the values of the coupling constants, two scenarios for the stationary behavior of a chain of interacting spasers may be realized: (1) all spasers are synchronized and oscillate with a unique phase or (2) a nonlinear autowave travels along the chain. In the latter scenario, the traveling wave is harmonic, unlike excitations in other known nonlinear systems. Due to the nonlinear nature of the system, any initial distribution of spaser states evolves into one of these steady states.

DOI: [10.1103/PhysRevB.85.165419](https://doi.org/10.1103/PhysRevB.85.165419)

PACS number(s): 73.20.Mf, 42.50.Nn, 78.67.Pt, 81.05.Xj

I. INTRODUCTION

In the last decade, quantum nanoplasmonics has experienced explosive growth due to numerous revolutionary applications in optics and optoelectronics (see Refs. 1–4 and references therein). The rapid emergence of this field reflects the increasing demands of nanotechnology. Nanoplasmonics utilizes outstanding optical properties of metal nanoparticles (NPs), which allow the electromagnetic field to be concentrated on a subwavelength scale. A combination of a nanoscale-active medium with the population inversion, e.g., a quantum dot (QD), and a metal NP results in the emergence of a nanoplasmonic counterpart of the laser–surface plasmon (SP) amplification by stimulated emission of radiation (spaser) first proposed by Bergman and Stockman⁵ and realized experimentally by Noginov *et al.*⁶ Schematically, the spaser is a system of inversely excited two-level QDs surrounding metal NPs.^{5,7} The principles of operation of the spaser are analogous to those for the laser, with the role of photons played by SPs localized at a NP.^{5,7–9} SPs are confined to a NP resembling a resonator. The spaser generates and amplifies the near field of the NP. SP amplification occurs due to nonradiative energy transfer from the QD to the NP. This process originates from the dipole–dipole (or other near field¹⁰) interaction between the QD and the plasmonic NP. This physical mechanism has high efficiency, because the probability of exciting the SP of $\sim (k_0 r)^{-3}$ exceeds the probability of radiative emission,¹¹ where r is the distance between the centers of the NP and the QD and k_0 is an optical wavenumber in vacuum. The generation of a large number of SPs induces the stimulated transition in the QD and further generation of SPs. Thus, the plasmonic mode is excited by pumping the QD. This process is inhibited by losses in the NP, which—together with pumping—results in undamped stationary oscillations of the spaser dipole moment.

A promising application of spasers is their use as inclusions in plasmonic metamaterials—composites with negative dielectric permittivity and magnetic permeability (for review, see Refs. 12 and 13). The inhibiting factor for applications of metamaterials is substantial joule loss due to the interaction of light with metal inclusions that fill metamaterials. This loss can be compensated by transforming metal inclusions into spasers inside metamaterials.^{14,15} Using spasers to compensate for

loss is promising but not straightforward. The problem is that above the generation threshold, the spaser is an autonomous (self-oscillating) system. Its dipole moment is excited not only by the external field but also by the field produced by the QD. Moreover, the dipole moment of the spaser's NP oscillates even in the absence of the external field. The frequency of this self-oscillation is determined by the plasmon frequency, the transition frequency of the QD, and characteristic times of relaxation of excitations in the NP and QD.⁹ Thus, a spaser is not necessarily synchronized with the external field. Nevertheless, as has been shown in Ref. 16, there is a domain (the Arnold tongue) of values of the external wave amplitude and the frequency detuning in which the spaser becomes synchronous with the driving wave and even exact compensation of losses can be achieved.¹⁷ This may lead to the creation of lossless metamaterials.

If spasers present in metamaterials are used to compensate for loss, we must understand the functioning of a system of interacting spasers distributed regularly or randomly in a dielectric matrix. In the present paper, we study a regular linear chain of interacting spasers. We demonstrate that, depending on the parameters of the system, two scenarios may be realized.

There are several papers devoted to the numerical simulation of electromagnetic wave traveling through a periodic system of spasers.^{18–21} In Refs. 18–21 a linear regime of interaction among spasers and between spasers and external optical wave has been studied. This linear regime arises when the probe pulse is so short that the population inversion does not change noticeably, or in a steady-state operation below the spasing threshold. This restriction makes it possible to describe the system in terms of the effective permittivity. Our study deals with the nonlinear regime in which the population inversion is above the spasing threshold.

The rest of the paper is organized as follows. In Sec. II, we briefly discuss main equations that describe operations of spasers. In Sec. III, we consider oscillations of two coupled spasers. In Secs. IV and V, we find solutions and analyze their stability for a model of a chain of spasers in which only neighboring NPs are coupled. Sec. VI deals with a more general model, in which the interaction of NPs with nearest QDs is included. This model is generalized further in Sec. VII to take into account the coupling of QDs that belong to neighboring spasers. Finally, Sec. VIII summarizes the paper.

II. OPERATION OF A SPASER: MAIN EQUATIONS

The simplest spaser consists of a two-level QD of radius r_{TLS} , which is positioned at a distance r from a metallic NP of radius r_{NP} . The whole system is immersed into a solid dielectric or semiconductor matrix with dielectric permittivity ε_M .⁵ Here, we discuss the excitation of the main (dipole) mode of the SP at a frequency ω_{SP} .

Following the theory of a usual one-atom, single-mode laser,²² the dynamics of the self-oscillating spaser can be described by the following Hamiltonian model:

$$\hat{H} = \hat{H}_{\text{SP}} + \hat{H}_{\text{TLS}} + \hat{V} + \hat{\Gamma}, \quad (1)$$

where

$$\hat{H}_{\text{SP}} = \hbar\omega_{\text{SP}}\hat{a}^\dagger\hat{a} \quad (2)$$

and

$$\hat{H}_{\text{TLS}} = \hbar\omega_{\text{TLS}}\hat{\sigma}^\dagger\hat{\sigma} \quad (3)$$

describe the energy of the electromagnetic field of the SP and of the QD, respectively^{5,13,23}; the operator $\hat{V} = -\hat{\boldsymbol{\mu}}_{\text{TLS}} \cdot \hat{\mathbf{E}}_{\text{NP}}$ determines the coupling between the QD and the NP; the operator $\hat{\Gamma}$ is responsible for relaxation and pumping²³; $\hat{a}(t)$ is the Bose operator of annihilation of the dipole SP; $\hat{\sigma} = |g\rangle\langle e|$ is the operator of the transition between the excited $|e\rangle$ and the ground $|g\rangle$ states of the QD; $\hat{\boldsymbol{\mu}}_{\text{TLS}} = \boldsymbol{\mu}_{\text{TLS}}(\hat{\sigma}(t) + \hat{\sigma}^\dagger(t))$ is the dipole moment of the QD; and $\boldsymbol{\mu}_{\text{TLS}} = \langle e|\mathbf{e}r|g\rangle$ is its off-diagonal matrix element.

The operator of the electric field has the form

$$\hat{\mathbf{E}}_{\text{NP}}(\mathbf{r}, t) = -A\nabla\varphi(\mathbf{r})(\hat{a}^\dagger + \hat{a}) = \frac{3(\mathbf{r}\boldsymbol{\mu}_{\text{NP}})\mathbf{r} - \boldsymbol{\mu}_{\text{NP}}r^2}{r^5}(\hat{a}^\dagger + \hat{a}), \quad (4)$$

where $A = (4\pi\hbar s/\varepsilon_d s')^{1/2}$, $s' = d(\text{Re}[s(\omega)])/d\omega|_{\omega=\omega_n}$, $s(\omega) = [1 - \varepsilon_{\text{NP}}(\omega)/\varepsilon_M(\omega)]^{-1}$, and φ is the potential of the SP dipole field, $\boldsymbol{\mu}_{\text{NP}} = \sqrt{3\hbar r_{\text{NP}}^3/(\partial\text{Re}\varepsilon_{\text{NP}}/\partial\omega)}\mathbf{e}_{\text{NP}}$ is the dipole moment of the NP.¹⁶ Since the SP wavelength λ_{SP} is much smaller than the optical wavelength in vacuum λ , we use the quasistatic approximation, in which the far fields are neglected. Thus, we find the frequency of the plasmonic resonance from the condition of existence of the nontrivial solution of the Laplace equation

$$\nabla\varepsilon(\mathbf{r})\nabla\varphi(\mathbf{r}) = 0,$$

in which $\varepsilon(\mathbf{r})$ equals ε_{NP} inside the NP and ε_M outside the NP in the dielectric matrix.

To separate the electromagnetic properties and the geometrical factor of the NP, it is convenient to represent the permittivity in the form⁵ $\varepsilon(\mathbf{r}) = (\varepsilon_{\text{NP}} - \varepsilon_M)(\Theta(\mathbf{r}) - s)$, where the step function $\Theta(\mathbf{r})$ defines the geometry of the problem: it is equal to zero in the dielectric matrix and equal to unity inside the NP, whereas $s = (1 - \varepsilon_{\text{NP}}/\varepsilon_M)^{-1}$ only depends on constitutive properties of the system. By using such notation, the Laplace equation may be written in the form^{8,9}

$$\nabla\Theta(\mathbf{r})\nabla\varphi(\mathbf{r}) = s\nabla^2\varphi(\mathbf{r}), \quad (5)$$

which allows us to find the eigenvalues s_n and eigenfunctions $\varphi_n(\mathbf{r})$, $n = 1, 2, \dots$. In a spherical NP, the n th plasmonic

multipole has the resonance at $\varepsilon_{\text{NP}} = -\varepsilon_M(n+1)/n$ and $s_n = n/(2n+1)$.^{11,13,24}

By taking into account the permittivity dispersion $\varepsilon_{\text{NP}}(\omega)$, the eigenfrequency Ω_n is determined from the condition $s(\Omega_n) = [1 - \varepsilon_{\text{NP}}(\Omega_n)/\varepsilon_M]^{-1} = s_n$. In general, due to joule losses in the metallic NP, the eigenfrequency has an imaginary part: $\Omega_n = \omega_n - i\gamma_n$. In addition, there are radiation losses of the NP due to the oscillation of a SP multipole. However, for small NPs (~ 30 nm), joule losses far exceed the loss due to radiation.^{13,25} This means that the spaser mainly generates the near field. For large NPs (~ 100 nm), the loss due to radiation dominates. This is the regime of the so-called dipole laser.²⁶ In this paper, we assume that the size of the NP is small and disregard the radiative losses.

For the quantization of the electromagnetic field, we take into account dispersion but neglect dissipation.²⁷ Losses and pumping are introduced into the final equations phenomenologically (see Ref. 26 for details).

Assuming that the frequency of the QD transition is close to the frequency of the plasmon resonance $\omega_{\text{SP}} \approx \omega_{\text{TLS}}$, we represent time dependencies of $\hat{a}(t)$ and $\hat{\sigma}(t)$ in the forms $\hat{a}(t) \equiv \hat{a}(t)e^{-i\omega t}$ and $\hat{\sigma}(t) \equiv \hat{\sigma}(t)e^{-i\omega t}$, where $\hat{a}(t)$ and $\hat{\sigma}(t)$ are slowly varying operators and ω is the spaser's self-oscillation frequency that we seek. In the approximation of the rotating wave,²² we neglect fast-oscillating terms, which are proportional to $\sim e^{\pm 2i\omega t}$. Then, the coupling operator can be written in the Jaynes-Cummings form²²

$$\hat{V} = \hbar\Omega_R(\hat{a}^\dagger\hat{\sigma} + \hat{\sigma}^\dagger\hat{a}), \quad (6)$$

where $\Omega_R = \frac{\boldsymbol{\mu}_{\text{NP}}\cdot\boldsymbol{\mu}_{\text{TLS}}-3(\boldsymbol{\mu}_{\text{NP}}\cdot\mathbf{e}_{\text{NP-TLS}})(\boldsymbol{\mu}_{\text{TLS}}\cdot\mathbf{e}_{\text{NP-TLS}})}{\hbar r^3}$ is the Rabi frequency, $\mathbf{e}_{\text{NP-TLS}}$ is unit vector pointing from the NP to the QD.^{16,26}

The commutation relations for operators $\hat{a}(t)$ and $\hat{\sigma}(t)$ are standard: $[\hat{a}, \hat{a}^\dagger] = \hat{1}$ and $[\hat{\sigma}^\dagger, \hat{\sigma}] = \hat{D}$, where the operator $\hat{D} = [\hat{\sigma}^\dagger, \hat{\sigma}] = \hat{n}_e - \hat{n}_g$ describes the population inversion of the ground states $\hat{n}_g = |g\rangle\langle g|$ and excited states $\hat{n}_e = |e\rangle\langle e|$, $\hat{n}_g + \hat{n}_e = \hat{1}$, of the QD. Using the Hamiltonian model, Eqs. (1)–(6), we obtain Heisenberg equations of motion for operators $\hat{a}(t)$, $\hat{\sigma}(t)$, and $\hat{D}(t)$.^{8,16,26}

$$\hat{D} = 2i\Omega_R(\hat{a}^\dagger\hat{\sigma} - \hat{\sigma}^\dagger\hat{a}) - \tau_D^{-1}(\hat{D} - \hat{D}_0), \quad (7)$$

$$\hat{\sigma} = (i\delta - \tau_\sigma^{-1})\hat{\sigma} + i\Omega_R\hat{a}\hat{D}, \quad (8)$$

$$\hat{a} = (i\Delta - \tau_a^{-1})\hat{a} - i\Omega_R\hat{\sigma}, \quad (9)$$

where $\delta = \omega - \omega_{\text{TLS}}$ and $\Delta = \omega - \omega_{\text{SP}}$ are frequency detunings. The terms with relaxation times $\propto \tau_D^{-1}$, τ_σ^{-1} , and τ_a^{-1} are introduced to account for the relaxation processes of the respective quantities. These relaxation times can be evaluated in terms of the macroscopic properties of the QD and NP. For a typical QD and silver NP, these values are^{28–32} $\tau_a^{-1} \sim 10^{14}\text{s}^{-1}$, $\tau_\sigma^{-1} \sim 10^{11}\text{s}^{-1}$, and $\tau_D^{-1} \sim 10^{13}\text{s}^{-1}$. The operator \hat{D}_0 describes pumping. The population inversion operator \hat{D}_0 plays the role of the operator \hat{D} in the regime of absence of generation. In other words, without generation, $\{\hat{D} = \hat{D}_0, \hat{a} = \hat{\sigma} = \hat{0}\}$ is a stable fixed point of Eqs. (7)–(9). When generation exists, this fixed point becomes unstable.^{22,23}

We neglect quantum fluctuations and correlations and consider $\hat{a}(t)$, $\hat{\sigma}(t)$, and $\hat{D}(t)$ as complex valued quantities

(c -numbers) so that we can use complex conjugation instead of Hermitian conjugation.^{5,26,33,34} The population inversion $D(t)$ must be a real valued quantity, because the respective operator is Hermitian. The quantities $\sigma(t)$ and $a(t)$ are the complex amplitudes of the dipole oscillations of the QD and SP, respectively.

As has been shown in Refs. 5 and 26, above the threshold pump level

$$D_{\text{th}} = \frac{1 + \Delta^2 \tau_a^2}{\Omega_R^2 \tau_a \tau_\sigma}, \quad (10)$$

the spaser oscillates with the frequency

$$\omega_a = \frac{\omega_{\text{SP}} \tau_a + \omega_{\text{TLS}} \tau_\sigma}{\tau_a + \tau_\sigma} \quad (11)$$

and Eqs. (7)–(9) have the stationary solutions

$$D = D_{\text{th}}, \quad (12)$$

$$\sigma = \frac{a}{\Omega_R} (\Delta + i \tau_a^{-1}), \quad (13)$$

$$a = \frac{e^{i\psi}}{2} \left(\frac{(D_0 - D_{\text{th}}) \tau_a}{\tau_D} \right)^{\frac{1}{2}}, \quad (14)$$

where ψ is an undetermined phase shift, whose value is immaterial. The frequency of the spaser's self-oscillations is always between the frequencies of the plasmon resonance and the QD transition. This is similar to frequency pulling, which is the well-known phenomenon in lasers. The square-root dependence of the amplitudes of dipole moments of metal NPs and QDs on pumping corresponds to the standard Hopf bifurcation at the creation of the limit cycle. In our approximation, the arising cycle is strictly circular, so even though spaser's self-oscillations are nonlinear, they are harmonic. As we show later, the nonlinear autowave of the spasing propagation is also harmonic.

III. SYNCHRONIZATION OF TWO SPASERS

The spaser, as a self-oscillating system, exhibits properties common to such systems. One that has been known as far back as Huygens is synchronization.³⁵ The synchronization may occur either under an action of the external force or due to the interaction of two self-oscillating systems. In both cases, we observe phase locking either when the system driven by an external harmonic field starts oscillating with the frequency of this field¹⁶ or when two coupled self-oscillating systems start oscillating in phase with the same frequency. The case of spaser synchronization by the external wave was considered in Ref. 16. In this section, we discuss synchronization of coupled spasers.

To describe behavior of two coupled spasers, we generalize the system of Eqs. (7)–(9) by introducing coupling terms:

$$\begin{aligned} \dot{\hat{D}}_1 &= 2i\Omega_{R1}(\hat{a}_1^\dagger \hat{\sigma}_1 - \hat{\sigma}_1^\dagger \hat{a}_1) + 2i\Omega_{\text{NP-TLS}}(\hat{a}_2^\dagger \hat{\sigma}_1 - \hat{\sigma}_1^\dagger \hat{a}_2) \\ &\quad + 2i\Omega_{\text{TLS-TLS}}(\hat{\sigma}_2^\dagger \hat{\sigma}_1 - \hat{\sigma}_1^\dagger \hat{\sigma}_2) - \tau_{D1}^{-1}(\hat{D}_1 - \hat{D}_{01}), \end{aligned} \quad (15)$$

$$\begin{aligned} \dot{\hat{D}}_2 &= 2i\Omega_{R2}(\hat{a}_2^\dagger \hat{\sigma}_2 - \hat{\sigma}_2^\dagger \hat{a}_2) + 2i\Omega_{\text{NP-TLS}}(\hat{a}_1^\dagger \hat{\sigma}_2 - \hat{\sigma}_2^\dagger \hat{a}_1) \\ &\quad + 2i\Omega_{\text{TLS-TLS}}(\hat{\sigma}_2^\dagger \hat{\sigma}_1 - \hat{\sigma}_1^\dagger \hat{\sigma}_2) - \tau_{D2}^{-1}(\hat{D}_2 - \hat{D}_{02}), \end{aligned} \quad (16)$$

$$\begin{aligned} \dot{\hat{\sigma}}_1 &= (i\delta - \tau_\sigma^{-1}) \hat{\sigma}_1 + i\Omega_{R1} \hat{a}_1 \hat{D}_1 + i\Omega_{\text{NP-TLS}} \hat{a}_2 \hat{D}_1 \\ &\quad + i\Omega_{\text{TLS-TLS}} \hat{\sigma}_2 \hat{D}_1, \end{aligned} \quad (17)$$

$$\begin{aligned} \dot{\hat{\sigma}}_2 &= (i\delta - \tau_\sigma^{-1}) \hat{\sigma}_2 + i\Omega_{R2} \hat{a}_2 \hat{D}_2 + i\Omega_{\text{NP-TLS}} \hat{a}_1 \hat{D}_2 \\ &\quad + i\Omega_{\text{TLS-TLS}} \hat{\sigma}_1 \hat{D}_2, \end{aligned} \quad (18)$$

$$\begin{aligned} \dot{\hat{a}}_1 &= (i\Delta - \tau_a^{-1}) \hat{a}_1 - i\Omega_{R1} \hat{\sigma}_1 - i\Omega_{\text{NP-NP}} \hat{a}_2 - i\Omega_{\text{NP-TLS}} \hat{\sigma}_2, \\ &\quad (19) \end{aligned}$$

$$\begin{aligned} \dot{\hat{a}}_2 &= (i\Delta - \tau_a^{-1}) \hat{a}_2 - i\Omega_{R2} \hat{\sigma}_2 - i\Omega_{\text{NP-NP}} \hat{a}_1 - i\Omega_{\text{NP-TLS}} \hat{\sigma}_1. \\ &\quad (20) \end{aligned}$$

Indexes 1 and 2 label the quantities corresponding to the first and second spasers, respectively;

$$\Omega_{\text{NP-NP}} = \frac{\boldsymbol{\mu}_{\text{NP1}} \cdot \boldsymbol{\mu}_{\text{NP2}} - 3(\boldsymbol{\mu}_{\text{NP1}} \cdot \mathbf{e}_{\text{NP-NP}})(\boldsymbol{\mu}_{\text{NP2}} \cdot \mathbf{e}_{\text{NP-NP}})}{\hbar r_{\text{NP-NP}}^3}$$

is a coupling constant between neighboring NPs;

$$\begin{aligned} \Omega_{\text{NP-TLS}} &= \frac{\boldsymbol{\mu}_{\text{NP1}} \cdot \boldsymbol{\mu}_{\text{TLS2}} - 3(\boldsymbol{\mu}_{\text{NP1}} \cdot \mathbf{e}_{\text{NP-TLS}})(\boldsymbol{\mu}_{\text{TLS2}} \cdot \mathbf{e}_{\text{NP-TLS}})}{\hbar r_{\text{NP-TLS}}^3} \\ &= \frac{\boldsymbol{\mu}_{\text{NP2}} \cdot \boldsymbol{\mu}_{\text{TLS1}} - 3(\boldsymbol{\mu}_{\text{NP2}} \cdot \mathbf{e}_{\text{NP-TLS}})(\boldsymbol{\mu}_{\text{TLS1}} \cdot \mathbf{e}_{\text{NP-TLS}})}{\hbar r_{\text{NP-TLS}}^3} \end{aligned}$$

is a coupling constant between the neighboring QD and the NP;

$$\begin{aligned} \Omega_{\text{TLS-TLS}} &= \frac{\boldsymbol{\mu}_{\text{TLS1}} \cdot \boldsymbol{\mu}_{\text{TLS2}} - 3(\boldsymbol{\mu}_{\text{TLS1}} \cdot \mathbf{e}_{\text{TLS-TLS}})(\boldsymbol{\mu}_{\text{TLS2}} \cdot \mathbf{e}_{\text{TLS-TLS}})}{\hbar r_{\text{TLS-TLS}}^3} \end{aligned}$$

is a coupling constant between neighboring QDs; $\mathbf{e}_{\text{NP-NP}}$, $\mathbf{e}_{\text{NP-TLS}}$, and $\mathbf{e}_{\text{TLS-TLS}}$ are unit vectors pointing from the NP to the neighboring NP, from the NP to the QD, and from the QD to the neighboring QD, respectively; and $r_{\text{NP-NP}}$, $r_{\text{NP-TLS}}$, and $r_{\text{TLS-TLS}}$ are the corresponding distances. These coupling constants have the dimension of frequency. For the typical QD and NP at optical frequencies of $\sim 5 \times 10^{15} \text{ s}^{-1}$, supposing that $r_{\text{NP-NP}}$, $r_{\text{NP-TLS}}$, $r_{\text{TLS-TLS}} \sim 50 \text{ nm}$, we obtain $\Omega_{\text{NP-NP}} \sim 10^{13} \text{ s}^{-1}$, $\Omega_{\text{NP-TLS}} \sim 10^{12} \text{ s}^{-1}$, and $\Omega_{\text{TLS-TLS}} \sim 10^{11} \text{ s}^{-1}$.

The values of the coupling constants depend on the orientation of corresponding dipoles. In particular, if the dipoles are parallel, then $\Omega_{1-2} = \gamma_i (\boldsymbol{\mu}_1 \cdot \boldsymbol{\mu}_2) / (\hbar r_{12}^3)$, with $\gamma_1 = -2$ for longitudinal and $\gamma_{2,3} = 1$ for transverse modes. Here, we imply that the γ factor is included in the definition of the coupling constants.

Similar to the case of a single spaser, for $D_0 < D_{\text{th}}$, where

$$D_{\text{th}} = \frac{1 + (\Omega_{\text{NP-NP}}^{\text{eff}} \tau_\sigma)^2}{(\Omega_R + 2\Omega_{\text{NP-TLS}})^2 \tau_a \tau_\sigma}, \quad (21)$$

only the trivial solution $a_{1,2} = 0$, $\sigma_{1,2} = 0$, $D_{1,2} = D_{01,2}$ satisfies the system of Eqs. (15)–(20). In Eq. (21), we introduce the notation $\Omega_{\text{NP-NP}}^{\text{eff}} = 2\Omega_{\text{NP-NP}} \tau_a / (\tau_a + \tau_\sigma)$. For $D_0 > D_{\text{th}}$, by direct substitution, we verify that if $\Omega_{\text{NP-TLS}} > 0$, then

$$\hat{a}_1 = \hat{a}_2, \quad \hat{\sigma}_1 = \hat{\sigma}_2, \quad \hat{D}_1 = \hat{D}_2, \quad (22a)$$

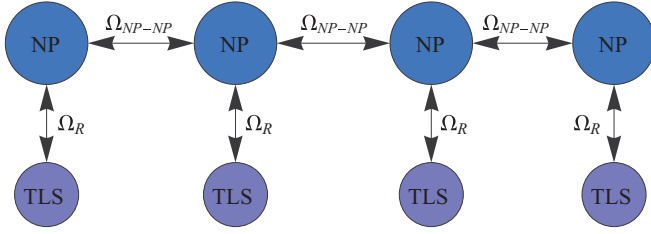


FIG. 1. (Color online) Schematic of the chain of spasers, in which neighboring NPs interact with each other.

is the stationary solution to Eqs. (15)–(20). For $\Omega_{NP-TLS} < 0$, the stationary solution is

$$\hat{a}_1 = -\hat{a}_2, \quad \hat{\sigma}_1 = -\hat{\sigma}_2, \quad \hat{D}_1 = \hat{D}_2. \quad (22b)$$

Thus, when pumping exceeds the threshold value (Eq. (21)), a couple of identical spasers behave like a single spaser for which the spasing occurs at the frequency

$$\omega = \Omega_{NP-NP}^{\text{eff}} + \frac{\omega_{SP}\tau_a + \omega_{TLS}\tau_\sigma}{\tau_a + \tau_\sigma}. \quad (23)$$

In this case, phase locking occurs so that the phase difference $\Delta\varphi$ between oscillations is equal either to zero or π if $\Omega_{NP-TLS} > 0$ or $\Omega_{NP-TLS} < 0$, respectively. This result is confirmed by our time-domain computer simulation showing that the system arrives at the stationary state given by Eqs. (21)–(23), independent of initial conditions.

IV. HAMILTONIAN MODEL OF A CHAIN OF SPASERS

In this section, we discuss a chain of spasers shown schematically in Fig. 1. As mentioned previously (see also Refs. 5 and 26), the main contribution to the interaction between the spaser's members, NPs and QDs, is due to near fields. At the first step, considering a linear chain of spasers, we take into account the dipole–dipole interaction Ω_{NP-NP} of NPs of the nearest-neighbor spasers, disregarding the far-field interaction—as well as the influence of the neighboring NP on the QD, which is considered in Sec. VI.

In the framework of the slowly varying envelope approximation $\hat{a}_n(t) \exp(-i\omega t)$, $\hat{\sigma}_n(t) \exp(-i\omega t)$, the Hamiltonian model of the chain of spasers with interacting NPs can be written as

$$\hat{H} = \sum_n \left(\hbar\omega_{SP}\hat{a}_n^+\hat{a}_n + \hbar\omega_{TLS}\hat{\sigma}_n^+\hat{\sigma}_n + \hbar\Omega_R(\hat{a}_n^+\hat{\sigma}_n + \hat{a}_n\hat{\sigma}_n^+) + \frac{1}{2}\hbar\Omega_{NP-NP}(\hat{a}_n^+\hat{a}_{n-1} + \hat{a}_n\hat{a}_{n-1}^+ + \hat{a}_n^+\hat{a}_{n+1} + \hat{a}_n\hat{a}_{n+1}^+) \right), \quad (24)$$

where the summation is performed over the spasers. The Heisenberg equations for the n th spaser can be written as

$$\hat{D}_n = 2i\Omega_R(\hat{a}_n^+\hat{\sigma}_n - \hat{\sigma}_n^+\hat{a}_n) - \tau_D^{-1}(\hat{D}_n - \hat{D}_{0n}), \quad (25)$$

$$\hat{\sigma}_n = (i\delta - \tau_\sigma^{-1})\hat{\sigma}_n + i\Omega_R\hat{a}_n\hat{D}_n, \quad (26)$$

$$\hat{a}_n = (i\Delta - \tau_a^{-1})\hat{a}_n - i\Omega_R\hat{\sigma}_n - i\Omega_{NP-NP}(\hat{a}_{n-1} + \hat{a}_{n+1}). \quad (27)$$

In Eq. (27), the last term is responsible for the spaser coupling.

Next, we replace operators with c -numbers and look for stationary solutions by considering the following equations:

$$2i\Omega_R(a_n^*\sigma_n - \sigma_n^*a_n) - \tau_D^{-1}(D_n - D_{0n}) = 0, \quad (28)$$

$$(i\delta - \tau_\sigma^{-1})\sigma_n + i\Omega_R a_n D_n = 0, \quad (29)$$

$$(i\Delta - \tau_a^{-1})a_n - i\Omega_R\sigma_n - i\Omega_{NP-NP}(a_{n-1} + a_{n+1}) = 0. \quad (30)$$

We assume that the solution of Eqs. (28)–(30) is a plane-traveling wave with a slowly varying amplitude: $a_n = a_{n,k} \exp(ikx)$ and $\sigma_n = \sigma_{n,k} \exp(ikx)$. Because x takes the discrete values $x = nb$, where b is the distance between nearest-neighbor spasers, we obtain

$$a_{n+1,k} = a_{n,k} \exp(ikb), \quad a_{n-1} = a_n \exp(-ikb). \quad (31)$$

Substituting these expressions into the system of Eqs. (28)–(30), we obtain a solution identical to the solution for the system of Eqs. (7)–(9) for a single spaser (for details, see Refs. 16 and 26) with the replacement

$$\Delta \rightarrow \Delta(k) - 2\Omega_{NP-NP} \cos kb. \quad (32)$$

In this case, $\Delta(k) = \omega_k - \omega_a$. The dispersion equation $\tau_a \Delta = -\tau_\sigma \delta$ of a solitary spaser,^{16,26} which results from Eqs. (7)–(9), now takes the form

$$\tau_a (\Delta(k) - 2\Omega_{NP-NP} \cos kb) = -\tau_\sigma \delta. \quad (33)$$

The solution to Eq. (33) gives us the dispersion equation

$$\omega_k = \omega_a + \Omega_{NP-NP}^{\text{eff}} \cos kb, \quad (34)$$

where the generation frequency of a single spaser ω_a is given by Eq. (11)²⁶ and ω_0 is the frequency of SPs. Thus, even though the chain of spasers is a nonlinear system, harmonic waves can travel in it. The dispersion equation for these waves is similar to the dispersion equation for the wave of dipole moments traveling along the linear system of the lossless chain of spherical particles in the absence of QDs.^{11,36,37} In the latter case, the dispersion equation for one longitudinal and two transverse modes has the form

$$\omega(k) = \omega_{SP} + (\gamma_i \omega_1^2 / \omega_{SP}) \cos kb. \quad (35)$$

As given earlier, $\gamma_1 = -2$ for longitudinal and $\gamma_{2,3} = 1$ for transverse modes. In Ref. 38, it was shown that $\omega_1^2 = r_{NP}^3 \omega_{pl}^2 / 3b^3$, where ω_{pl} is the plasmon frequency in the Drude type of dispersion $\varepsilon_{NP} = 1 - \omega_{pl}^2 / \omega^2$. Taking into account that $|\mu_{NP}| = \sqrt{3\hbar r_{NP}^3} / (\partial \text{Re} \varepsilon_{NP} / \partial \omega)$ and the assumption² that SP resonance occurs at $\omega_{SP} = \omega_{pl} / \sqrt{3}$, the factor in Eq. (34) can be recast as

$$\begin{aligned} \Omega_{NP-NP}^{\text{eff}} &= 2\Omega_{NP-NP} \frac{\tau_a}{\tau_a + \tau_\sigma} \\ &= \frac{2\tau_a}{\tau_a + \tau_\sigma} \gamma_i \frac{\mu_{NP}^2}{\hbar b^3} = \frac{\tau_a}{\tau_a + \tau_\sigma} \gamma_i \frac{\omega_1^2}{\omega_{SP}}, \end{aligned}$$

which up to the factor $\tau_a / (\tau_a + \tau_\sigma)$ coincides with the factor in Eq. (35). In the absence of the QD, we can put $\tau_\sigma = 0$ and arrive at the exact coincidence.

Thus, the dispersion equations for the harmonic waves traveling along a chain of plasmonic NPs and a chain of nonlinear spasers are nearly the same. Setting τ_σ equal to zero makes ω_a equal to ω_{SP} and $\Omega_{NP-NP}^{\text{eff}}$ in Eq. (34) equal to the factor ω_1^2 / ω_{SP} in Eq. (35). However, there is a principal

difference between the waves in these systems. In the linear system, the wave amplitude can take an arbitrary value, whereas in the nonlinear case, the amplitude is determined by pumping:

$$a_{n,k} = \frac{1}{2} \exp(i\varphi) \times \sqrt{[D_0 - (1 + (\Omega_{\text{NP-NP}}^{\text{eff}} \tau_\sigma)^2 \cos^2 kb) / \Omega_R^2 \tau_a \tau_\sigma] \frac{\tau_a}{\tau_\sigma}}. \quad (36)$$

In the linear case, we can have a superposition of waves: two or more waves can travel simultaneously. Their amplitudes and wavenumbers are determined by initial conditions. That is not the case for the nonlinear system. In the nonlinear system, regardless of the initial conditions, the threshold value D_{th} of the inversion of population, for which the wave can arise, depends on the wavenumber k :

$$D_{\text{th}} = \frac{1 + (\Delta - 2\Omega_{\text{NP-NP}} \cos kb)^2 \tau_a^2}{\Omega_R^2 \tau_a \tau_\sigma} = \frac{1 + (\Omega_{\text{NP-NP}}^{\text{eff}} \tau_\sigma)^2 \cos^2 kb}{\Omega_R^2 \tau_a \tau_\sigma}. \quad (37)$$

In terms of the frequency, this relation can be written as

$$D_{\text{th}} = \frac{1 + (\omega_a - \omega_k)^2 \tau_a \tau_\sigma}{\Omega_R^2 \tau_a \tau_\sigma}. \quad (38)$$

The value of D_{th} has its minimum at $\omega_k = \omega_a$, and the corresponding wavenumber is equal to $k = \pi/2b$. The wave with this frequency and wavenumber is the first to be generated. We assume that only this wave survives and the other waves transfer their energy to this one. To confirm the assumption,

let us consider how a small disturbance affects a nonlinear harmonic wave.

Equations (34) and (35) are valid for $k > k_0$ only. For $k < k_0$, the waves become leaky. As we mentioned in Sec. I, the radiation is suppressed for $(k_0 r_{\text{NT-TLS}})^{-3} \ll 1$. However, when k is smaller than k_0 , k^{-1} becomes the new length scale of the system so that the efficiency of the radiative emission $(k_0/k)^{-3} \geq 1$ becomes substantial, suppressing SP amplification.

V. ANALYSIS OF STABILITY

The solution to Eqs. (28)–(30) has the form

$$D_{\text{st}}(k) = D_{\text{th}}(k) = \frac{1 + (\Omega_{\text{NP-NP}}^{\text{eff}} \tau_\sigma)^2 \cos^2 kb}{\Omega_R^2 \tau_a \tau_\sigma}, \quad (39)$$

$$a_{\text{st}}(k) = \frac{e^{i\psi}}{2} \sqrt{(D_0 - D_{\text{th}}(k)) \frac{\tau_a}{\tau_D}}, \quad (40)$$

$$\begin{aligned} \sigma_{\text{st}} &= a_{\text{st}} (\Delta - 2\Omega_{\text{NP-NP}} \cos kb + i/\tau_a) / \Omega_R \\ &= a_{\text{st}} (i - \Omega_{\text{NP-NP}}^{\text{eff}} \tau_\sigma \cos kb) / \tau_a \Omega_R, \end{aligned} \quad (41)$$

with $k(\omega)$ determined by Eq. (35).

To verify the stability of this solution, we add to it a disturbance of the form $\exp(\Lambda_\chi t + i\chi x)$. Here $x = bn$, n is a spaser's number, χ is the wavenumber of the disturbance, and Λ_χ is the increment of growth of this disturbance. We consider the initial autowave to be stable if for any χ we obtain $\text{Re}\Lambda_\chi < 0$. To proceed, it is convenient to rewrite the system of Eqs. (25)–(27) in a vector form:

$$\dot{\mathbf{u}} = \mathbf{f}(\mathbf{u}), \quad (42)$$

where

$$\mathbf{u} = \begin{pmatrix} A_1 \\ A_2 \\ S_1 \\ S_2 \\ D \end{pmatrix}, \quad \mathbf{f}(\mathbf{u}) = \begin{pmatrix} -\tau_a^{-1} A_1 + \Omega_{\text{NP-NP}}^{\text{eff}} \tau_\sigma \tau_a^{-1} A_2 \cos kb + \Omega_R S_2 \\ -\Omega_{\text{NP-NP}}^{\text{eff}} \tau_\sigma \tau_a^{-1} A_1 \cos kb - \tau_a^{-1} A_2 - \Omega_R S_1 - \Omega_1 \\ -\tau_\sigma^{-1} S_1 - \delta \cdot S_2 - \Omega_R A_2 D \\ \delta \cdot S_1 - \tau_\sigma^{-1} S_2 + \Omega_R A_1 D + \Omega_2 D \\ 4\Omega (A_2 S_1 - A_1 S_2) - 4\Omega_2 S_2 - \tau_D^{-1} (D - D_0) \end{pmatrix}. \quad (43)$$

The following notations were introduced: $A_1 = \text{Re}a_n$, $A_2 = \text{Im}a_n$, $S_1 = \text{Re}\sigma_n$, and $S_2 = \text{Im}\sigma_n$.

The equilibrium position \mathbf{u}_0 of vector \mathbf{u} is defined by Eqs. (33), (34), and (36). We shift vector \mathbf{u}_0 by $\delta\mathbf{u} \exp(\Lambda_\chi t + i\chi x)$, and then after linearization, we obtain

$$\delta\dot{\mathbf{u}} = \Lambda_\chi \delta\mathbf{u} = \hat{M} \delta\mathbf{u}, \quad (44)$$

where the matrix \hat{M} is

$$\hat{M} = \frac{1}{\tau_a} \begin{pmatrix} -1 & \Omega_{\text{NP-NP}}^{\text{eff}} \tau_\sigma \cos \chi b & 0 & \Omega_R \tau_a & 0 \\ -\Omega_{\text{NP-NP}}^{\text{eff}} \tau_\sigma \cos \chi b & -1 & -\Omega_R \tau_a & 0 & 0 \\ 0 & -\Omega_R \tau_a D_{\text{st}} & -\tau_a \tau_\sigma^{-1} & -\tau_a \delta & -\Omega_R \tau_a A_{2st} \\ \Omega_R \tau_a D_{\text{st}} & 0 & \delta \tau_a & -\tau_a \tau_\sigma^{-1} & \Omega_R \tau_a A_{1st} \\ -4\Omega_R \tau_a S_{2st} & 4\Omega_R \tau_a S_{1st} & 4\Omega_R \tau_a A_{2st} & -4\Omega_R \tau_a A_{1st} & -\tau_a \tau_D^{-1} \end{pmatrix}. \quad (45)$$

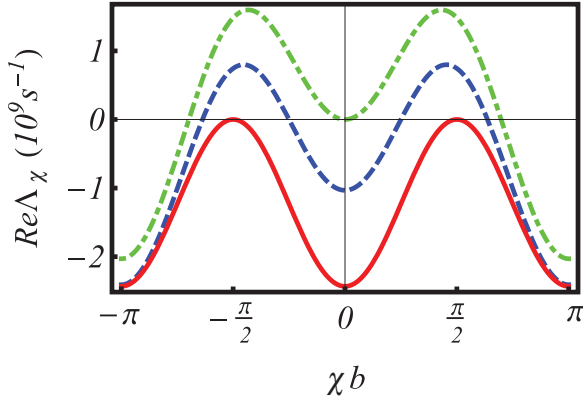


FIG. 2. (Color online) Dependencies of maximum values of $\text{Re}\Lambda_\chi$ on χ for different values of k : dashed, dot-dashed, and solid lines correspond to $kb = 0, \pi/4$, and $\pi/2$, respectively. $\Omega_{\text{NP-NP}} = 10^{13} \text{s}^{-1}$.

As it follows from Eq. (44), the solution (the autowave) with a given k is stable if real parts of all eigenvalues of \hat{M} are negative for any χ . In Fig. 2, the dependencies of maximum values of $\text{Re}\Lambda_\chi$ on χ for different values of k are shown. We can see that all values of $\text{Re}\Lambda_\chi$ are negative for $kb = \pi/2$ only. This confirms our assumption that only the wave arising for the minimum value of D_{th} is stable.

To make sure that for any initial condition the autowave with $k = \pi/2b$ survives, we solve the nonlinear system of Eqs. (25)–(27) numerically. We consider a chain of $N = 100$ spasers with periodic boundary conditions. We take into account the interaction with nearest neighbors only, so the first spaser interacts with the second and the hundredth ones. With the accuracy of computer simulation, we learn that for any initial conditions, the stationary solution corresponds to one of two waves, with $k = \pm\pi/2b$ and $\omega = \omega_{\text{SP}}$. The existence of two solutions is due to the inversion invariance ($x \rightarrow -x$) of the system (see Ref. 39 and references therein).

In the linear case of a NP chain, if we express the initial condition as a sum of harmonic waves, each harmonic has a fixed value of the Poynting vector. Then, each harmonic generates two waves with the same $\omega(k)$ traveling in opposite directions and the sum of Poynting vectors equal to the initial one. Ultimately, a number of harmonic waves can travel simultaneously. The total number is determined by the initial conditions.

In our nonlinear case of a spaser chain, any initial condition evolves into a single wave whose direction of propagation depends on the initial conditions. The total Poynting vector of the initial state determines the direction of propagation of a single surviving wave.

In the case considered in this section, there are no stable solutions with $kb = 0$ and $kb = \pm\pi$. Thus, in a chain in which spasers are coupled via interaction of NPs only, the synchronous oscillations of spasers do not occur.

VI. TURNING ON NP–QD COUPLING OF NEIGHBORING SPASERS

Up to this point, we have assumed that there is a coupling between nearest NPs only. The QDs have been affected by the

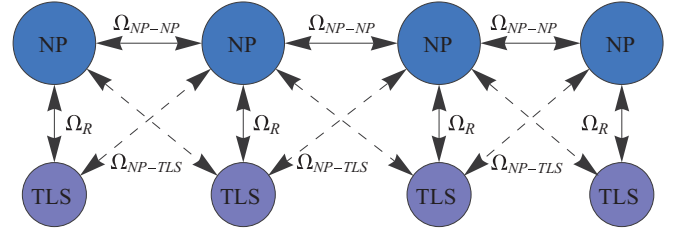


FIG. 3. (Color online) Schematic of the chain of spasers, in which each NP interacts with NPs and QDs of neighboring spasers.

field of their own NPs. Now we take into account the influence of the nearest NPs on QDs. For simplicity, the symmetric case, in which the coupling consists of interaction of a QD with neighboring NPs, $\Omega_{\text{NP-TLS}}$ is the same but may differ from the coupling constant between the QD and the NP, forming a single spaser Ω_R (Fig. 3).

The Hamiltonian model of such a system can be written as

$$\begin{aligned} \hat{H} = & \sum_n (\hbar\omega_{\text{SP}}\hat{a}_n^\dagger\hat{a}_n + \hbar\omega_{\text{TLS}}\hat{\sigma}_n^\dagger\hat{\sigma}_n + \hbar\Omega_R(\hat{a}_n^\dagger\hat{\sigma}_n + \hat{a}_n\hat{\sigma}_n^\dagger) \\ & + 1/2 \cdot \hbar\Omega_{\text{NP-NP}}(\hat{a}_n^\dagger\hat{a}_{n-1} + \hat{a}_n\hat{a}_{n-1}^\dagger + \hat{a}_n^\dagger\hat{a}_{n+1} + \hat{a}_n\hat{a}_{n+1}^\dagger) \\ & + 1/2 \cdot \hbar\Omega_{\text{NP-TLS}}(\hat{\sigma}_n^\dagger\hat{a}_{n-1} + \hat{\sigma}_n\hat{a}_{n-1}^\dagger + \hat{\sigma}_n^\dagger\hat{a}_{n+1} \\ & + \hat{\sigma}_n\hat{a}_{n+1}^\dagger)), \end{aligned} \quad (46)$$

and the equations for slow variation in time amplitudes for the n th spaser are

$$\begin{aligned} \dot{\hat{D}}_n = & 2i\Omega_R(\hat{a}_n^\dagger\hat{\sigma}_n - \hat{\sigma}_n^\dagger\hat{a}_n) + 2i\Omega_{\text{NP-TLS}}(\hat{a}_{n-1}^\dagger\hat{\sigma}_n - \hat{\sigma}_n^\dagger\hat{a}_{n-1}) \\ & + 2i\Omega_{\text{NP-TLS}}(\hat{a}_{n+1}^\dagger\hat{\sigma}_n - \hat{\sigma}_n^\dagger\hat{a}_{n+1}) - \tau_D^{-1}(\hat{D}_n - \hat{D}_{0n}), \end{aligned} \quad (47)$$

$$\begin{aligned} \dot{\hat{\sigma}}_n = & (i\delta - \tau_\sigma^{-1})\hat{\sigma}_n + i\Omega_R\hat{a}_n\hat{D}_n + i\Omega_{\text{NP-TLS}}\hat{a}_{n-1}\hat{D}_n \\ & + i\Omega_{\text{NP-TLS}}\hat{a}_{n+1}\hat{D}_n, \end{aligned} \quad (48)$$

$$\begin{aligned} \dot{\hat{a}}_n = & (i\Delta - \tau_a^{-1})\hat{a}_n - i\Omega_R\hat{\sigma}_n - i\Omega_{\text{NP-TLS}}\hat{\sigma}_{n-1} \\ & - i\Omega_{\text{NP-TLS}}\hat{\sigma}_{n+1} - i\Omega_{\text{NP-NP}}(\hat{a}_{n-1} + \hat{a}_{n+1}). \end{aligned} \quad (49)$$

If we look for solutions of Eqs. (47)–(49) in the form of the traveling wave, $a_n(t) = a_{n,k} \exp(ikx)$, $\sigma_n(t) = \sigma_{n,k} \exp(ikx)$, and $D_n(t) = D_{n,k} \exp(ikx)$, with $x = nb$, then these equations can be recast as

$$\begin{aligned} \dot{\hat{D}}_n = & 2i(\Omega_R + 2\Omega_{\text{NP-TLS}} \cos kb)(\hat{a}_n^\dagger\hat{\sigma}_n - \hat{\sigma}_n^\dagger\hat{a}_n) \\ & - \tau_D^{-1}(\hat{D}_n - \hat{D}_{0n}), \end{aligned} \quad (50)$$

$$\dot{\hat{\sigma}}_n = (i\delta - \tau_\sigma^{-1})\hat{\sigma}_n + i(\Omega_R + 2\Omega_{\text{NP-TLS}} \cos kb)\hat{a}_n\hat{D}_n, \quad (51)$$

$$\begin{aligned} \dot{\hat{a}}_n = & (-i\Omega_{\text{NP-NP}}^{\text{eff}}\tau_\sigma\tau_a^{-1} \cos kb - \tau_a^{-1})\hat{a}_n \\ & - i(\Omega_R + 2\Omega_{\text{NP-TLS}} \cos kb)\hat{\sigma}_n. \end{aligned} \quad (52)$$

Comparing the system of Eqs. (50)–(52) with Eqs. (25)–(27), we can see that accounting for the QD interaction with neighboring NPs results in change of the coupling constant Ω_R and the frequency detuning Δ . Instead of Ω_R and Δ , we have $\Omega_R^{\text{eff}}(k) = \Omega_R + 2\Omega_{\text{NP-TLS}} \cos kb$ and $\Delta(k) = \Delta - 2\Omega_{\text{NP}} \cos kb = -\Omega_{\text{NP-NP}}^{\text{eff}}\tau_\sigma\tau_a^{-1} \cos kb$, respectively. The stationary solution of

Eqs. (50)–(52) is

$$D_{\text{st}} = D_{\text{th}} = \frac{1 + (\Omega_{\text{NP-NP}}^{\text{eff}} \tau_{\sigma})^2 \cos^2 kb}{[\Omega_R^{nn}(k)]^2 \tau_a \tau_{\sigma}}, \quad (53)$$

$$a_{\text{st}} = \frac{e^{i\psi}}{2} \sqrt{(D_0 - D_{\text{th}}) \tau_a \tau_D^{-1}}, \quad (54)$$

$$\sigma_{\text{st}} = a_{\text{st}} (i \tau_a^{-1} - (\Omega_{\text{NP-NP}}^{\text{eff}} \tau_{\sigma}) \cos kb / \tau_a) / \Omega_R^{nn}(k). \quad (55)$$

Let us check the stability of this solution. The matrix \hat{M} , which appears in the preceding linear stability analysis, is modified as follows:

$$\begin{pmatrix} -\tau_a^{-1} & \Omega_{\text{NP-NP}}^{\text{eff}} \tau_{\sigma} \cos \chi b / \tau_a & 0 & \Omega_R^{nn}(\chi) & 0 \\ -\Omega_{\text{NP-NP}}^{\text{eff}} \tau_{\sigma} \cos \chi b / \tau_a & -\tau_a^{-1} & -\Omega_R^{nn}(\chi) & 0 & 0 \\ 0 & -\Omega_R^{nn}(\chi) D_{\text{st}} & -\tau_{\sigma}^{-1} & -\delta & -\Omega_R^{nn}(\chi) A_{2\text{st}} \\ \Omega_R^{nn}(\chi) D_{\text{st}} & 0 & \delta & -\tau_{\sigma}^{-1} & \Omega_R^{nn}(\chi) A_{1\text{st}} \\ -4\Omega_R^{nn}(\chi) S_{2\text{st}} & 4\Omega_R^{nn}(\chi) S_{1\text{st}} & 4\Omega_R^{nn}(\chi) A_{2\text{st}} & -4\Omega_R^{nn}(\chi) A_{1\text{st}} & -\tau_D^{-1} \end{pmatrix}. \quad (56)$$

Again, the solution is stable if the real parts of all eigenvalues of the matrix \hat{M} are negative. The form of the stable solution depends on the sign of the coupling constant Ω_R . Let us first consider $\Omega_R > 0$. For $\Omega_{\text{NP-TLS}} = 0$, the situation is identical to the one discussed previously: the stable wave has the wavenumber $kb = \pi/2$. Nonzero $\Omega_{\text{NP-TLS}} > 0$ results in a decrease of the wavenumber of the stable solution. In particular, for $\Omega_{\text{NP-TLS}} = 4 \times 10^{10} \text{s}^{-1}$, the stable wave has $kb = 1.2$. A further increase of the coupling constant results in a decrease of the wavenumber until it reaches zero at some value of $\Omega_{\text{NP-TLS}}^*$ (Fig. 4). Beyond this point, the wavenumber remains zero when $\Omega_{\text{NP-TLS}}$ increases.

The threshold value $\Omega_{\text{NP-TLS}}^*$ can be evaluated by taking into account that the pumping threshold for the stable wave has the minimum value. Equation (53) shows that if $\omega_{\text{SP}} = \omega_{\text{TLS}}$, then

$$D_{\text{th}}(k) = \frac{1 + (\tau_{\sigma} \Omega_{\text{NP-NP}}^{\text{eff}})^2 \cos^2 kb}{(\Omega_R + 2\Omega_{\text{NP-TLS}} \cos kb)^2 \tau_a \tau_{\sigma}}. \quad (57)$$

The values of k corresponding to minimum and maximum values of this expression are determined by the equations

$$\sin kb = 0, \quad (58)$$

$$\cos kb = \frac{2\Omega_{\text{NP-TLS}}}{(\tau_{\sigma} \Omega_{\text{NP-NP}}^{\text{eff}})^2 \Omega_R}. \quad (59)$$

A real solution of Eq. (59) exists only when the right-hand part is smaller than unity. In this case, we can show that when the inequality $2\Omega_{\text{NP-TLS}}(\tau_{\sigma} \Omega_{\text{NP-NP}}^{\text{eff}})^{-2} \leq \Omega_R$ is satisfied, solutions of Eqs. (58) and (59) correspond to maximum and minimum values of $D_{\text{th}}(k)$, respectively. If $2\Omega_{\text{NP-TLS}}(\tau_{\sigma} \Omega_{\text{NP-NP}}^{\text{eff}})^{-2} > \Omega_R$, the minimum of $D_{\text{th}}(k)$ is achieved for wavenumbers given by the solutions of Eq. (58). This means that

$$\Omega_{\text{NP-TLS}}^* = \frac{1}{2} (\tau_{\sigma} \Omega_{\text{NP-NP}}^{\text{eff}})^2 \Omega_R. \quad (60)$$

For negative values of $\Omega_{\text{NP-TLS}}$, a similar analysis shows that for $-\Omega_{\text{NP-TLS}}^* \leq \Omega_{\text{NP-TLS}} \leq 0$, the minimum of $D_{\text{th}}(k)$ is given by the solutions of Eq. (59); for $\Omega_{\text{NP-TLS}} \leq -\Omega_{\text{NP-TLS}}^*$, it is achieved for $kb = \pi$. To summarize, in the case of $\Omega_R > 0$, the dependence of the wavenumber of the stable solution on the coupling constant $\Omega_{\text{NP-TLS}}$ is

$$kb = \begin{cases} \pi, \Omega_{\text{NP-TLS}} < -\Omega_{\text{NP-TLS}}^* \\ \cos^{-1} \left(\frac{2\Omega_{\text{NP-TLS}}}{(\tau_{\sigma} \Omega_{\text{NP-NP}}^{\text{eff}})^2 \Omega_R} \right), & -\Omega_{\text{NP-TLS}}^* \leq \Omega_{\text{NP-TLS}} \leq \Omega_{\text{NP-TLS}}^* \\ 0, \Omega_{\text{NP-TLS}} > \Omega_{\text{NP-TLS}}^* \end{cases}. \quad (61)$$

Similarly, for $\Omega_R < 0$,

$$kb = \begin{cases} 0, \Omega_{\text{NP-TLS}} < -\Omega_{\text{NP-TLS}}^* \\ \pi - \cos^{-1} \left(\frac{2\Omega_{\text{NP-TLS}}}{(\tau_{\sigma} \Omega_{\text{NP-NP}}^{\text{eff}})^2 \Omega_R} \right), & -\Omega_{\text{NP-TLS}}^* \leq \Omega_{\text{NP-TLS}} \leq \Omega_{\text{NP-TLS}}^* \\ \pi, \Omega_{\text{NP-TLS}} > \Omega_{\text{NP-TLS}}^* \end{cases}. \quad (62)$$

The dependencies given by Eqs. (61) and (62) are shown in Fig. 5(a) and 5(b), respectively.

Thus, depending on the value of the coupling constant between a NP and the neighboring QD, $\Omega_{\text{NP-TLS}}$, two types of excitations in a chain of spasers arise: (1) for

$\Omega_{\text{NP-TLS}} < \Omega_{\text{NP-TLS}}^*$, a harmonic autowave travels in the system, and (2) for $\Omega_{\text{NP-TLS}} > \Omega_{\text{NP-TLS}}^*$, there are no propagating solutions and all spasers oscillate in phase for positive spaser coupling $\Omega_R > 0$; if $\Omega_R < 0$, the spasers oscillate in antiphase.

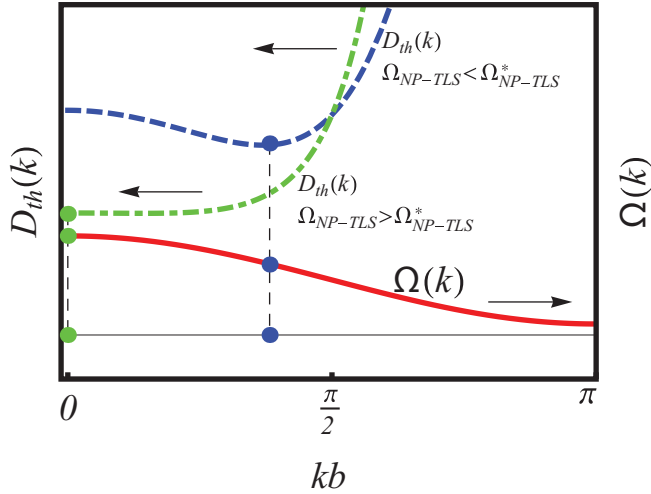


FIG. 4. (Color online) Dependence of threshold pumping on the wavenumber k for $\Omega_{\text{NP-TLS}} < \Omega_{\text{NP-TLS}}^*$ (dashed curve) and $\Omega_{\text{NP-TLS}} > \Omega_{\text{NP-TLS}}^*$ (dot-dashed curve). The solid curve shows the dependence $\omega(k)$.

VII. TURNING ON THE QD-QD INTERACTION

In this section, we show that taking into account the interaction of QDs belonging to neighboring spasers does not substantially change the physical picture. For simplicity, we assume symmetric NP-QD coupling. All interactions between spasers are shown schematically in Fig. 6.

The new Hamiltonian model can be written as

$$\begin{aligned} \hat{H} = & \sum_n [\hbar\omega_{\text{SP}}\hat{a}_n^+\hat{a}_n + \hbar\omega_{\text{TLS}}\hat{\sigma}_n^+\hat{\sigma}_n + \hbar\Omega_R(\hat{a}_n^+\hat{\sigma}_n + \hat{a}_n\hat{\sigma}_n^+) \\ & + \frac{1}{2}\hbar\Omega_{\text{NP-NP}}(\hat{a}_n^+\hat{a}_{n-1} + \hat{a}_n\hat{a}_{n-1}^+ + \hat{a}_n^+\hat{a}_{n+1} + \hat{a}_n\hat{a}_{n+1}^+) \\ & + \frac{1}{2}\hbar\Omega_{\text{NP-TLS}}(\hat{\sigma}_n^+\hat{a}_{n-1} + \hat{\sigma}_n\hat{a}_{n-1}^+ + \hat{\sigma}_n^+\hat{a}_{n+1} + \hat{\sigma}_n\hat{a}_{n+1}^+) \\ & + \frac{1}{2}\hbar\Omega_{\text{TLS-TLS}}(\hat{\sigma}_n^+\hat{\sigma}_{n-1} + \hat{\sigma}_n\hat{\sigma}_{n-1}^+ + \hat{\sigma}_n^+\hat{\sigma}_{n+1} + \hat{\sigma}_n\hat{\sigma}_{n+1}^+)], \end{aligned} \quad (63)$$

where $\Omega_{\text{TLS-TLS}}$ is the QD-QD coupling constant. Following the procedure described in previous sections, we arrive at the equations of motion of the spasers:

$$\begin{aligned} \dot{\hat{D}}_n = & 2i(\Omega_R + 2\Omega_{\text{NP-TLS}} \cos kb)(\hat{a}_n^+\hat{\sigma}_n - \hat{a}_n\hat{\sigma}_n^+) \\ & - (\hat{D}_n - \hat{D}_{0n})\tau_D^{-1}, \end{aligned} \quad (64)$$

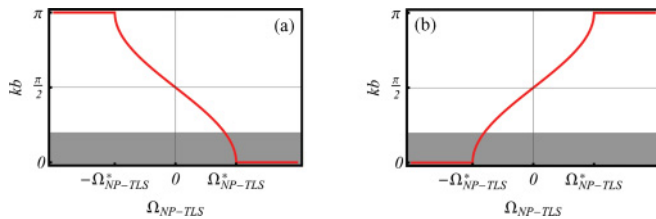


FIG. 5. (Color online) Dependencies of the stable solution of Eqs. (50)–(52) for (a) $\Omega_R > 0$ and (b) $\Omega_R < 0$, respectively. The shaded areas correspond to leaky wave solutions (see the comment at the end of Sec. IV).

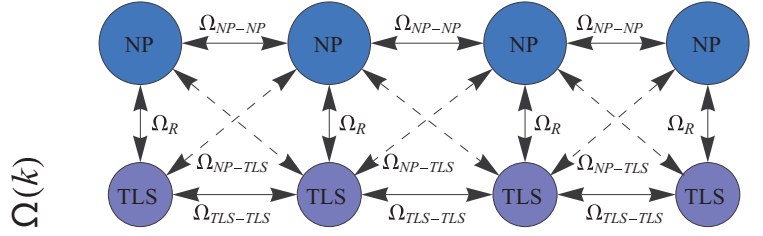


FIG. 6. (Color online) Schematic of the chain of spasers, in which each NP and QD interacts with NPs and QDs of neighboring spasers.

$$\begin{aligned} \dot{\hat{\sigma}}_n = & (i\delta - \tau_\sigma^{-1})\hat{\sigma}_n + i(\Omega_R + 2\Omega_{\text{NP-TLS}} \cos kb)\hat{a}_n\hat{D}_n \\ & + 2i\Omega_{\text{TLS-TLS}}\hat{\sigma}_n\hat{D}_n \cos kb, \end{aligned} \quad (65)$$

$$\begin{aligned} \dot{\hat{a}}_n = & -[(1 + i\Omega_{\text{NP-NP}}^{\text{eff}}\tau_\sigma \cos kb)\tau_a^{-1}]\hat{a}_n \\ & - i(\Omega_R + 2\Omega_{\text{NP-TLS}} \cos kb)\hat{\sigma}_n. \end{aligned} \quad (66)$$

This system of equation has a stationary solution; the frequency of spasing is defined by the equation

$$\begin{aligned} \omega^2 \frac{2\Omega_{\text{TLS-TLS}}\tau_a}{(\Omega_R + 2\Omega_{\text{NP-TLS}} \cos kb)^2} \\ + \omega \left(\tau_a + \tau_\sigma - \frac{4\Omega_{\text{TLS-TLS}}\tau_a(\omega_{\text{NP}} + 2\Omega_{\text{NP-NP}} \cos kb)}{(\Omega_R + 2\Omega_{\text{NP-TLS}} \cos kb)^2} \right) \\ + \frac{2\Omega_{\text{TLS-TLS}}\tau_a((\omega_{\text{NP}} + 2\Omega_{\text{NP-NP}} \cos kb)^2 + \tau_a^{-2})}{(\Omega_R + 2\Omega_{\text{NP-TLS}} \cos kb)^2} \\ - \omega_{\text{TLS}}\tau_\sigma - (\omega_{\text{SP}} + 2\Omega_{\text{NP-NP}} \cos kb)\tau_a = 0. \end{aligned} \quad (67)$$

$\Omega_{\text{TLS-TLS}}$ is much smaller than all other coupling constants, because the respective dipole moments are smaller and the distance is larger. Equation (67) has two solutions. We have to choose the one that tends to the solutions of Eqs. (52) and (53) as $\Omega_{\text{TLS-TLS}}$ tends to zero. For this solution, neglecting higher-order terms in $\Omega_{\text{TLS-TLS}}$, we obtain the dispersion equation

$$\begin{aligned} \omega(k) = & \omega_a + \Omega_{\text{NP-NP}}^{\text{eff}} \cos kb \\ & + \frac{2\Omega_{\text{TLS-TLS}}\tau_a}{(\tau_a + \tau_\sigma)(\Omega_R + 2\Omega_{\text{NP-TLS}} \cos kb)^2} \\ & \times [(\omega_a - \omega_{\text{SP}} - \Omega_{\text{NP-NP}}^{\text{eff}}\tau_\sigma\tau_a^{-1} \cos kb)^2 + \tau_a^{-2}]. \end{aligned} \quad (68)$$

For the threshold value of the inversion, we obtain

$$D_{\text{st}} = D_{\text{th}} = \frac{1 + (\Omega_{\text{NP-NP}}^{\text{eff}}\tau_\sigma)^2 \cos^2 kb}{(\Omega_R + 2\Omega_{\text{NP-TLS}} \cos kb)^2 \tau_a \tau_\sigma}, \quad (69)$$

where $\Delta = \omega(k) - \omega_{\text{NP}}$. Both $\omega(k)$ and $D_{\text{th}}(k)$ depend on $\cos kb$ only. The result of the differentiation of Eq. (69) with respect to k is $\sin kb$ multiplied by a function that has no zeros if $\Omega_{\text{NP-TLS}} > \Omega_{\text{NP-TLS}}^*$. Therefore, extrema of $D_{\text{th}}(k)$ are achieved for $kb = 0$ and $kb = \pi$ depending upon the sign of the second derivative, which is the same as in Sec. VI for small values of $\Omega_{\text{TLS-TLS}}$. Thus, when coupling between two QDs is “turned on” and the NP-QD coupling constant is larger than the threshold value, $\Omega_{\text{NP-TLS}}^*$, the wave numbers of the stable solution are still either $kb = 0$ or $kb = \pi$ depending upon the sign of Ω_R . However, the value of $\Omega_{\text{NP-TLS}}^*$ is different from the

one given by Eq. (60). In the case when $\Omega_{\text{NP-TLS}} < \Omega_{\text{NP-TLS}}^*$, the dependence $k(\Omega_{\text{NP-TLS}})$ is similar to that for $\Omega_{\text{NP-TLS}} = 0$.

VIII. SUMMARY

In this paper, we have studied excitations in a chain of interacting spasers. We have shown that, depending on the strength of the interaction between a QD and the nearest NP, either a synchronized oscillation of all spasers or a harmonic autowave traveling along the chain may arise. Thus, the pumped QD may either excite its own spasers so that all spasers are synchronized or, cooperating with the other QDs, excite a plasmonic wave traveling along the chain. This is the wave of NP polarization whose dispersion is similar to that predicted in Refs. 2 and 11 for linear systems. Unlike the general case of a wave propagating in a nonlinear lattice,³⁹ the nonlinear character of the spasers' response to an external field results neither in soliton nor in kink solutions. Rather, the response is a perfectly harmonic wave. However, unlike harmonic waves in linear systems, in a chain of spasers, (1) the wave has a fixed value of the wavenumber, which is

determined by the minimum value of the pumping threshold and the values of the coupling constants; (2) its amplitude has a fixed value, which is determined by the pumping strength; and (3) its propagation direction is determined by the initial conditions.

The results obtained are valid for synchronized waves with wavenumbers greater than an optical wavenumber in the surrounding space. If $k < k_0$, the waves become leaky, radiative emission becomes substantial, and lasing would be initiated in the spaser.⁴⁰

ACKNOWLEDGMENTS

The authors are indebted to J. B. Pendry, who drew our attention to the possibility of the stationary excitation at the chain of spasers in the form of a traveling wave. This work was supported by Russian Foundation for Basic Research Grants No. 10-02-91750, No. 10-02-92115, No. 11-02-92475, and No. 12-02-01093 and by a PSC-CUNY grant.

*alexander.lisyansky@qc.cuny.edu

¹S. V. Gaponenko, *Introduction to Nanophotonics* (Cambridge University Press, New York, 2010).

²S. A. Maier, *Plasmonics: Fundamentals and Applications* (Springer, New York, 2007).

³V. M. Shalaev and S. Kawata (eds.), *Nanophotonics with Surface Plasmons* (Elsevier, Amsterdam, 2007).

⁴Z. M. Wang and A. Neogi (eds.), *Nanoscale Photonics and Optoelectronics* (Springer, Berlin, 2010).

⁵D. J. Bergman and M. I. Stockman, *Phys. Rev. Lett.* **90**, 027402 (2003).

⁶M. A. Noginov, G. Zhu, A. M. Belgrave, R. Bakker, V. M. Shalaev, E. E. Narimanov, S. Stout, E. Herz, T. Suteewong, and U. Wiesner, *Nature* **460**, 1110 (2009).

⁷M. I. Stockman, *Nat. Photon.* **2**, 327 (2008).

⁸K. Li, X. Li, M. I. Stockman, and D. J. Bergman, *Phys. Rev. B* **71**, 115409 (2005).

⁹M. I. Stockman, *J. Opt.* **12**, 024004 (2010).

¹⁰I. R. Gabitov, B. Kennedy, and A. I. Maimistov, *IEEE J. Sel. Top. Quantum Electron.* **16**, 401 (2010).

¹¹V. V. Klimov, *Phys. Usp.* **51**, 839 (2008).

¹²W. Cai and V. Shalaev, *Optical Metamaterials: Fundamentals and Applications* (Springer, Dordrecht, 2010).

¹³L. Novotny and B. Hecht, *Principles of Nano-Optics* (Cambridge University Press, New York, 2006).

¹⁴M. I. Stockman, *Phys. Rev. Lett.* **106**, 156802 (2011).

¹⁵M. I. Stockman, *Phil. Trans. R. Soc. A* **369**, 3510 (2011).

¹⁶E. S. Andrianov, A. A. Pukhov, A. V. Dorofeenko, A. P. Vinogradov, and A. A. Lisyansky, *Opt. Express* **19**, 24849 (2011).

¹⁷E. S. Andrianov, A. A. Pukhov, A. V. Dorofeenko, A. P. Vinogradov, and A. A. Lisyansky, *Opt. Lett.* **36**, 4302 (2011).

¹⁸M. Wegener, J. L. García-Pomar, C. M. Soukoulis, N. Meinzer, M. Ruther, and S. Linden, *Opt. Express* **16**, 19785 (2008).

¹⁹A. Fang, T. Koschny, M. Wegener, and C. M. Soukoulis, *Phys. Rev. B* **79**, 241104(R) (2009).

²⁰A. Fang, T. Koschny, and C. M. Soukoulis, *J. Opt.* **12**, 024013 (2010).

²¹S. Wuestner, A. Pusch, K. L. Tsakmakidis, J. M. Hamm, and O. Hess, *Phys. Rev. Lett.* **105**, 127401 (2010).

²²M. O. Scully and M. S. Zubairy, *Quantum Optics* (Cambridge University Press, Cambridge, UK, 1997).

²³R. H. Pantell and H. E. Puthoff, *Fundamentals of Quantum Electronics* (Wiley, New York, 1969).

²⁴V. S. Zuev and G. Y. Zueva, *Opt. Spectrosc.* **107**, 614 (2009).

²⁵E. S. Andrianov, A. A. Pukhov, A. V. Dorofeenko, A. P. Vinogradov, and A. A. Lisyansky, *Phys. Rev. B* **85**, 035405 (2012).

²⁶I. E. Protsenko, A. V. Uskov, O. A. Zaimidoroga, V. N. Samoilov, and E. P. O'Reilly, *Phys. Rev. A* **71**, 063812 (2005).

²⁷P. W. Milonni, *The Quantum Vacuum: An Introduction to Quantum Electrodynamics* (Academic Press, Boston, 1994).

²⁸A. K. Sarychev and G. Tartakovsky, *Phys. Rev. B* **75**, 085436 (2007).

²⁹F. Stietz, J. Bosbach, T. Wenzel, T. Vartanyan, A. Goldmann, and F. Träger, *Phys. Rev. Lett.* **84**, 5644 (2000).

³⁰T. S. Sosnowski, T. B. Norris, H. Jiang, J. Singh, K. Kamath, and P. Bhattacharya, *Phys. Rev. B* **57**, R9423 (1998).

³¹M. Bayer and A. Forchel, *Phys. Rev. B* **65**, 041308 (2002).

³²J. M. Harbold, H. Du, T. D. Krauss, K.-S. Cho, C. B. Murray, and F. W. Wise, *Phys. Rev. B* **72**, 195312 (2005).

³³A. N. Lagarkov, A. K. Sarychev, V. N. Kissel, and G. Tartakovsky, *Phys. Usp.* **52**, 959 (2009).

³⁴A. S. Rosenthal and T. Ghannam, *Phys. Rev. A* **79**, 043824 (2009).

³⁵A. Pikovsky, M. Rosenblum, and J. Kurths, *Synchronization: A Universal Concept in Nonlinear Sciences* (Cambridge University Press, Cambridge, UK, 2001).

³⁶M. Quinten, A. Leitner, J. R. Krenn, and F. R. Aussenegg, *Opt. Lett.* **23**, 1331 (1998).

³⁷I. V. Zabkov, V. V. Klimov, I. V. Treshin, and O. A. Glazov, *Quantum Electron.* **41**, 742 (2011).

³⁸M. L. Brongersma, J. W. Hartman, and H. A. Atwater, *Phys. Rev. B* **62**, R16356 (2000).

³⁹A. Scott, *Nonlinear Science* (Oxford University Press, New York, 2003).

⁴⁰N. I. Zheludev, S. L. Prosvirnin, N. Papanikolaou, and V. A. Fedotov, *Nat. Photon.* **2**, 351 (2008).